Asian Journal of Information Technology 6 (9): 981-985, 2007
ISSN: 1682-3915

Diagnostic and Detection Rotor Faults in Induction Machines

[1]T. Bahi, [2]D. Bouneb, [1]A. Ourici and [3]G. Barakat
[1]Loboratory of LASA, Department of Electrotechnic, Faculty of Sciences Engineering,
Badji Mokhtar University, Sidi Amar, Annaba 23000, Algeria
[2]Department Electrotechnic, Faculty of Sciences Engineering, Skikda University, Algeria
[3]GREAH, University du Havre, BP 540, 76058 Le Havre, France

Abstract: In this study, authors gives a monitoring technique of broken rotor bar and ring detection of squirrel cage induction motors. For diagnosis, we proposed model of squirrel cage induction motors under rotor faults where the machine inductances are calculated by means of the magnetic energy stored in the air gap. Diagnostic information is found in the spectrum of stator current. The current waveforms is analysed using Fast Fourier Transform (FFT). The rotor fault is manifested as an increase in the amplitude of the 2sf and other spectral components. Simulation test results show agreement between the healthy and faults machine.

Key words: Induction motors, diagnosis, rotor fault, modelling

INTRODUCTION

Induction motors are critical components for electric utilities and process industries. However, it is becoming increasingly important to use condition monitoring techniques to give early warning of imminent failure. Many of motor faults have an electrical reason (Szabo *et al*., 2004). Although rotor bar faults covers approximately 10% of overall fault conditions in squirrel cage induction motors (Cardaso *et al*., 1995).

Hence, for several years, many monitoring algorithm have been proposed in literature (Benbouzid, 2000; Legowski *et al*., 1996). Amongst the various diagnostic methods used recently and mainly those using a data base containing information related to the various faults and issued from the spectral analysis of several motor quantities such as stator currents, instantaneous stator power and electromagnetic torque. The current stator approach requires only a current sensor, able to give a clear picture of the picture of the stator current.

The conventional indicator of the broken rotor bar in the single phase of motor current spectrum is well recognized by sidebands displaced by 2sf [Hz] around the mains peak at full load working conditions with high slip, where f is the supply frequency and s is the motor slip.

The objective of this study, is to develop a model of squirrel cage induction motor extended to the general case of faults. The proposed model is based on a coupled magnetic circuit (Hsu, 1995). The expressions of the different magnetizing inductances and mutual inductances are derived from the stored magnetic energy in the air gap unlike the widely used method based on the air gap flux across the windings. The stored magnetic energy in the air gap is calculated using the winding functions theory and a previously developed doubly slotted air gap permeance model (Ostavic, 1989). The rotor bar resistances as well as the rotor end ring resistances depend on the rotor speed with conventional formulas.
In practice, motor load may not be steady and if current is sampled when the motor load changes, sidebands may not be additional currents of the (1±2s).f frequency and the same amplitude, in the stator. These induced currents depend only on the operating conditions and motor's initial (Liao and Lipo, 1994). New component of the stator current at frequency (1-2s).f is a reaction of the initial component with at frequency, induced by the stator current spectrum is the sum of the too components at frequency (1-2s).f . The new component of stator current at frequency (1+2s).f is also visible in the spectra of stator current. A rotating magnetic field continues to produce the stator current components (Houdouin *et al*., 1997) at frequencies (1±2ks). f, with k=1, 2, 3 ….

Finally, some simulation results illustrate the proposed model in the case of healthy machine and broken bars rotor faults.

Corresponding Author: Tahar Bahi, Loboratory of LASA, Department of Electrotechnic, Faculty of Sciences Engineering, Badji Mokhtar University, Sidi Amar, Annaba 23000, Algeria

CIRCUIT MODELLING UNDER ROTOR FAULTS

A squirrel cage three phase motor is considered, its rotor is composed of N_b isolated bars, uniformly distributed on the rotor surface and short circuited with two rings (Bennouza *et al.*, 2006). Each rotor bar and end ring segment are characterized by a resistance and inductance.

The rotor is described in the terms of loops as shown in Fig. 1.

The model considered in replacing the q bars squirrel cage by an equivalent circuit containing q+1 magnetically coupled meshes. The current in each mesh of the rotor cage is an independent variable. Classical assumptions are to be considered such as infinite permeability of iron as well as no inter-bar currents. With these assumptions, the system of differential equations describing the behavior of induction machine with m stator phases and q rotor bars can be written in vector-matrix form and in a compact manner as follows (Houdouin *et al.*, 2001, 2002).

$$\begin{cases} \dfrac{d}{dt}[I] = -[L]^{-1}.\left([R]+\Omega\dfrac{d[L]}{d\theta}\right).[I]+[L]^{-1}[V] \\ \dfrac{d\Omega}{dt} = \dfrac{1}{2J}[I]^t\left\{\dfrac{d[L]}{d\theta}\right\}[I]-\dfrac{f}{J}\Omega-\dfrac{1}{J}T_L \\ \dfrac{d\theta}{dt} = \Omega \end{cases} \quad (1)$$

Where:

[R] and [L] are the resistances and the inductances matrices, respectively;

The current vector [I] and the voltage [V] can be expressed as:

$$[I]^t = \left[[I_s]^t[I_r]^t\right] = \left[[i_{s1}.....i_{sm}]^t[i_{r1}\ .....\ i_{rq}\ i_e]^t\right] \quad (2)$$

$$[V]^t = \left[[V_s]^t[0]^t\right] = \left[[v_{s1}\ \ v_{s2}\ v_{s3}.....v_{sm}]^t[0]^t\right] \quad (3)$$

Where, t represent the transpose of a vector; T_L and J are the load torque and the inertia moment of the machine respectively.

The mutual inductance between winding "I" and winding "j" is expressed by following formulae.

$$L_{ij}(\theta) = \frac{1}{\mu_0}\int_0^{L_{ax}}\int_0^{2\pi} F_{wi}(\theta,\theta_s,z).F_{wj}(\theta,\theta_s,z).e(\theta,\theta_s,z)\,P^2(\theta,\theta_s,z).R_{av}(\theta,\theta_s,z).d\theta_s.dz \quad (4)$$

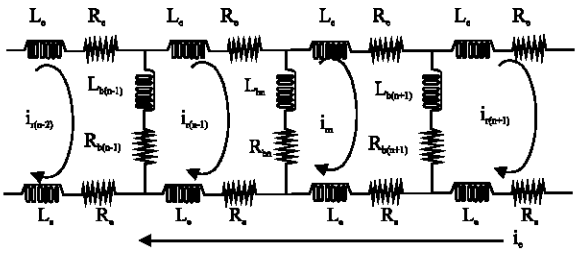

Fig. 1: Rotor cage equivalent circuit

Where, L_{ax} is the effective airgap axial length; e (θ, θ_s, z): is the effective air-gap function and R_{av} (θ, θ_s, z) is the average radius of the air-gap given by:

$$R_{av}(\theta,\theta_s,z) = R_r + e(\theta,\theta_s,z)/2 \quad (5)$$

The functions F_{wi} (θ, θ_s, z) and F_{wj} (θ, θ_s, z) are the winding functions of winding "i" is the winding functions of winding "j", respectively. Also, P (θ,θ_s, *z*) is the air gap permeance function.

The broken rotor bars is modeled by an equivalent circuit containing q+1 magnetically coupled meshes. Practically, the rotor bars are numbered from 1 to q either a bar is broken or not and their state is saved (broken or healthy). In order to define the rotor meshes, one searches the first healthy bars which constitute the first bar of the first mesh. The following healthy bar is the second bar of the first mesh. The second and following rotor meshes are constructed in the same manner. Consequently, if mesh "k" is constituted by bar "i" and bar "j" separated by n_{bb} consecutive broken bars, the resistance of mesh 'k' is given by:

$$R_k = 2.R_b + 2.(n_{bb}+1).R_e \quad (6)$$

And the total inductance of mesh 'k' is:

$$L_{mkk} = L_{rkk} + 2.L_{cb} + 2.(n_{bb}+1).L_{ce} \quad (7)$$

Where, L_{rkk} is the magnetizing inductance of the mesh "k". Also, the mutual inductance between mesh "k" and the end ring become:

$$L_{mke} = (n_{bb}+1).L_{ce} \quad (8)$$

Obviously, the new dimension of system (1) is obtained by subtracting the total number of broken bars from its dimension in the healthy case (m+q+1). The mutual inductances between rotor meshes on one side and between rotor meshes and stator phases on the other

side are calculated by means of expression (2) with the use of adequate winding functions for meshes containing broken bars.

In the same manner, the end rings are numbered from 1 to q either an end ring is broken or not and their state is saved (broken or healthy). When a broken end ring occurs, the corresponding cage mesh in the healthy case is included in the ring mesh. So, if n_{ber} designates an adequate number of broken end rings, the resistance of the ring mesh is expressed by:

$$R_{mr} = q.R_e + n_{ber}.R_b \quad (9)$$

The number n_{ber} must de determined by an adequate algorithm based on the different changes in the cage circuit induced by the broken end rings. A similar algorithm is used to determine the magnetizing and leakage inductances of the cage meshes and the ring mesh which total inductance is expressed by:

$$L_{mee} = 2.L_{\sigma b} + 2.(n_{bb} + 1).L_{\sigma e} + \sum_k L_{rkk} \quad (10)$$

The L_{rkk}, are the magnetizing inductances corresponding to the meshes containing a broken end ring and which belong now to the ring mesh.

RESULTS AND DISCUSSION

Simulation is carried out using a motor having the following parameters: 4 Kw, 230/400v, 14.2/8.2 A, 2840 rpm, 2 poles, 24 stator slots, 30 rotor bars.

Simulation results of a healthy machine are shown in Fig. 2. In this study case, the simulation has been carried out using a torque of 15 Nm. Where the machine speeds up over a time of 0.5 s approximately and then it settles to the running speed. During the start up the torque oscillates and then settles to the required load torque.

Figure 2c shows a phase current of the stator of the present case study. Fourier analysis of this current signal shows clearly the presence of the fundamental at 50 Hz frequency of the supply (Fig. 2d). In Alpha_Beta plan shown in Fig. 2e the signal describes a condensed plot around the centre. The circular shape in the plan indicates that the machine is without fault i.e. healthy.

In this case study the machine parameters have been simulated under the condition of broken bars in the rotor.

Figure 3a shows that the speed does not have a significant difference because of the machine inertia. Whereas the oscillations recorded in the steady state of the plot illustrates clearly the presence of a fault (Fig. 3b). The analysis of the phase current signal in Fig. 3c shows clearly the presence of a harmonic order at a frequency of

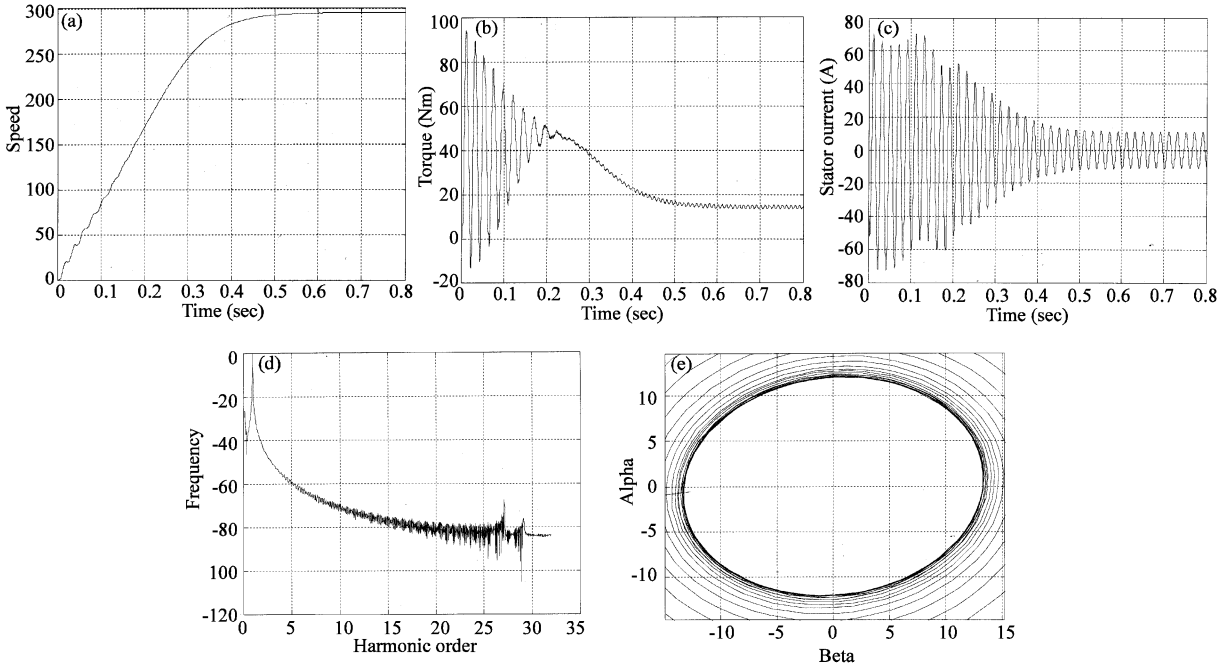

Fig. 2: Behaviour of a healthy machine during start up

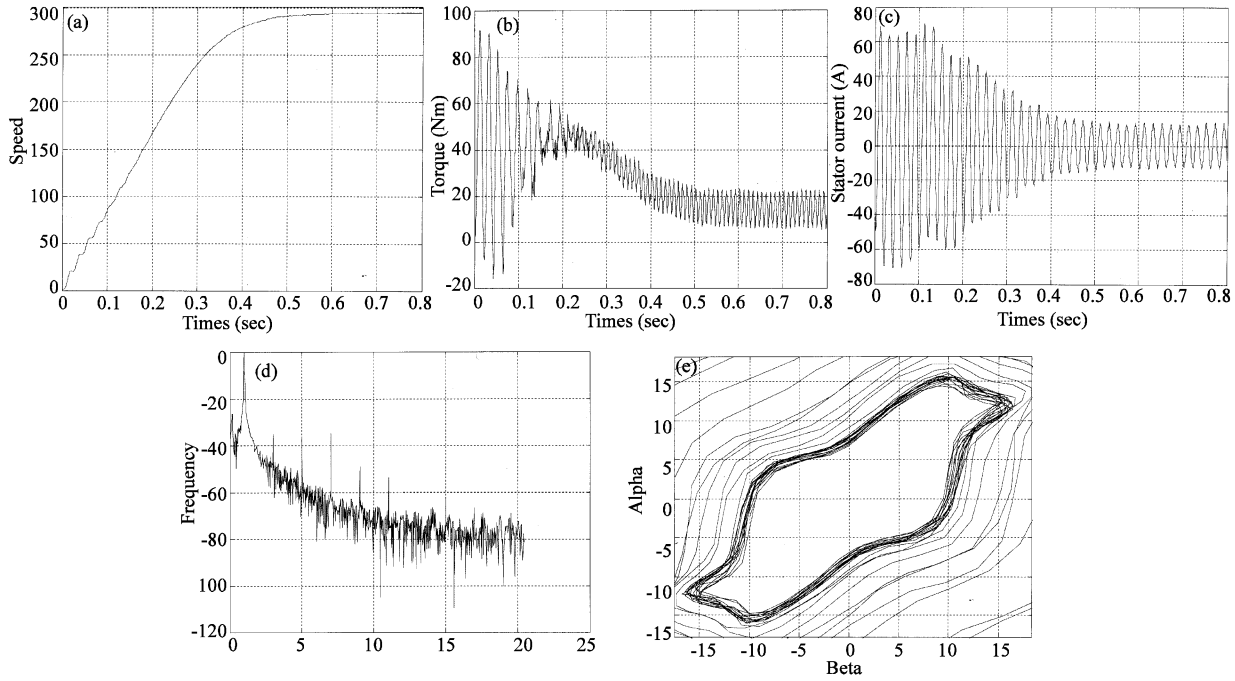

Fig. 3: The machine parameters under the condition of broken bars in the rotor

$(1\pm2s)f_1$ as stated previously (Fig. 3d). In this case study its representation in the Alph_Beta plan the shape is not exactly circular anymore, as in the case of a healthy machine. Its zigzag shape is shown in Fig. 3e.

CONCLUSION

In this study, a winding function theory based global model for the simulation of faulty induction machines under stator and rotor faults was presented. An approach based one the drowning of the Concordia current components for the monitoring of induction motor by computer is being used. However, the interest of the used technique lies in the possibility to detect bars fault in the possibility to detect bars fault by the distortion of the Concordia current components leads to an alpha-beta's vector. The inductances calculation based on magnetic energy considerations was exposed and the numerical storage of inductances was discussed. The simulated results show that rotor cage faults can effectively detected by the proposed approach.

REFERENCES

Benbouzid, M.E.H., 2000. A review of induction motors signature analysis as a medium for faults detection. IEEE. Trans. Ind. Elec., 47: 984-993.

Benouzza, N., M. Zerikat and A. Benetton, 2006. Squirrel Cage Rotor Faults Detection In Induction motor Utilizing Advanced Park's Vectors Approach. International conference on control, Modeling and Diagnostis, Annaba, Algeria.

Cardoso, A.J.M. *et al*., 1995. Rotor cage fault diagnosis in three-phase induction motors, by Park's vector approach. 30th Ind. Applic Soc. Ann. Meeting, Orlando, Florida, pp: 642-646.

Houdouin, G., G. Barakat, B. Dakyo and E. Destobbeleer, 2001. An improved method for dynamic simulation of air-gap eccentricity in induction machines. In: Proc. IEEE. SDEMPED, Grado, Italy, pp: 133-138.

Houdouin, G., G. Barakat, B. Dakyo and E. Destobbeleer, 2002. A Method for the simulation of inter-turn short circuits in squirrel cage induction machines. In: Proc. of EPE-PEMC, Caveat and Dubrovnik, Croatia.

Houdouin, G., G. Barakat, T. Derrey and E. Destobbeleer, 1997. A simple analytical model for the calculation of harmonics due to slotting in the airgap flux density waveform of an electrical machine. In: Proc. EPE, Trondheim, Norway, 2: 2601-2605.

Hsu, J.S., 1995. Monitoring of defects in induction motors through air-gap torque observation. IEEE. Trans. Ind. Applicat., 31: 1016-1021.

Legowski, S.F., A.H.M. Sadrul Ula and A.M. Trzynadlowski, 1996. Instantaneaous stator power as a medium for the signature analysis of induction motors. IEEE. Trans. Ind. Application, 32: 904-909.

Liao, Y. and T.A. Lipo, 1994. Effect of saturation third harmonic on the induction machine performance. Elect. Mach. Power Sys., 22: 155-171.

Ostovic, V., 1989. Dynamics of Saturated Electric Machines. Springer-Verlag, New York.

Szabo, L., J.B. Dobai and K.A. Biro, 2004. Rotor faults detection in squirrel cage induction motors by current signature analysis. International Conference on Automation, Quality and Testing Robotics, Cluj-Napoca, Romania.